Improvement of magnetocrystalline anisotropy of columnar structure for epitaxially grown CoCr-based perpendicular media

doi: 10.1063/1.1558093

Improvement of magnetocrystalline anisotropy of columnar structure for epitaxially grown CoCr-based perpendicular media

Shin Saito,[a] Norikazu Itagaki, Fumikazu Hoshi, and Migaku Takahashi
Department of Electronic Engineering, Graduate School of Engineering, Tohoku University, Sendai 980-8579, Japan

(Presented on 14 November 2002)

To improve uniaxial magnetic anisotropy K_u^{grain} of *c*-plane-oriented columnar grains for CoCr-based perpendicular recording media, an epitaxial growth technique has been applied. The main results are as follows. (1) Using a Ru(3 nm) or $Co_{60}Cr_{40}$(20 nm)/C(1 nm) intermediate layer, K_u^{grain} for a $Co_{69}Cr_{19}Pt_8B_4$ medium was enhanced from 2.04×10^6 erg/cm^3 to 2.53×10^6 erg/cm^3 or to 2.76×10^6 erg/cm^3, respectively. (2) The enhancement of K_u^{grain} depends on the composition of the magnetic layer when using the $Co_{60}Cr_{40}$/C intermediate layer. (3) The epitaxial growth technique is also effective to increase $K_u^{\text{grain}}V_{\text{act}}/kT$. Especially, in the media with a high concentration of B or Cr, the thermal stability is improved mainly due to an increase of K_u^{grain} rather than an enlargement of V_{act}. © *2003 American Institute of Physics.* [DOI: 10.1063/1.1558093]

To improve the thermal stability of high density recording for CoCr-based perpendicular media, it is essential to use materials with high uniaxial magnetocrystalline anisotropy energy, K_u^{grain}. We have reported that epitaxial growth of a $Co_{69}Cr_{19}Pt_8B_4$ magnetic layer by utilizing a $Co_{60}Cr_{40}$/C intermediate layer is effective to improve K_u^{grain} of *c*-plane-oriented columnar grains and eliminate the formation of an initial growth layer. In this study, the influence of magnetic layer and intermediate layer materials on K_u^{grain} of epitaxially grown media is further investigated.

CoCrPt and CoCrPtB perpendicular thin film media were fabricated by a dc magnetron sputtering method on 65 mm diam glass disk substrates using the so-called ultraclean sputtering system.[1] The substrate temperature was varied from 150 to 350 °C and was optimized such that the perpendicular coercivity of the media takes maximum. The film thickness of the media was varied from 5 to 50 nm. The underlayer and the protective layer were 25-nm-thick Ti, and 7-nm-thick C.

The crystal structure of the media was examined by the grazing incident angle x-ray diffraction (XRD) method (in-plane XRD; $2\theta_\chi$ scan) using Cu $K\alpha$ radiation.[2] The incident angle was fixed at 0.4°, which corresponds to about a 20-nm-thick penetration of the x ray from the incident surface. The saturation magnetization M_s and perpendicular magnetic anisotropy $K_{u\perp}^{\text{exp}}$ were evaluated by a vibrating sample magnetometer (VSM) and high sensitive torque magnetometer, respectively. The uniaxial magnetocrystalline anisotropy of columnar grains, K_u^{grain}, and the initial layer thickness, d_{ini}, were derived by perpendicular magnetic torque curve and determined from the $K_{u\perp}^{\text{exp}}\times d_{\text{mag}}$ versus d_{mag} plot.[3,4] Activation volume V_{act}, which corresponds with the coherent magnetic reversal volume in a medium, was determined by irreversible susceptibility measurement using the following equations:[5] $V_{\text{act}}=(kT)/(M_sH_f)$, $H_f=-[dH_r(t)/d\ln(t)]$, where H_f is the fluctuation field, T is the absolute temperature, and k is the Boltzmann's constant. H_f was determined by linear extrapolation of the H_r versus $\ln(t)$ plot.

To realize the epitaxial growth of the magnetic layer, the intermediate layer, which consists of *c*-plane-oriented hexagonal grains, Ru or $Co_{60}Cr_{40}$/C(1 nm), was selected. Here, a 1 nm carbon seedlayer underlying the $Co_{60}Cr_{40}$ intermediate layer plays a very important role to form Cr-deprived hcp grains with Cr segregation structure in the $Co_{60}Cr_{40}$ layer without forming σ-phase grains.[6,7]

Figure 1 (left) shows the dependence of perpendicular magnetic properties H_c and S for 30-nm-thick $Co_{69}Cr_{19}Pt_8B_4$ media on intermediate layer thickness, d_{inter}, of (A) Ru and

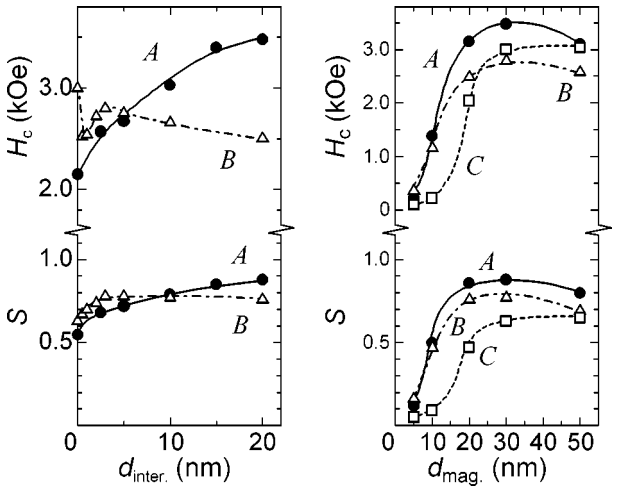

FIG. 1. Left: dependence of perpendicular magnetic properties H_c and S for 30-nm-thick $Co_{69}Cr_{19}Pt_8B_4$ media on intermediate layer thickness, d_{inter}, of (A) Ru, and (B) $Co_{60}Cr_{40}$/C(1 nm), respectively. Right: dependence of H_c and S on magnetic film thickness, d_{mag}, for $Co_{69}Cr_{19}Pt_8B_4$ media (A) with Ru(3 nm), (B) with $Co_{60}Cr_{40}$(20 nm)/C(1 nm), and (C) without an intermediate layer, respectively.

[a]Electronic mail: ssaito@ecei.tohoku.ac.jp
[b]Also at: New Industry Creation Hatchery Center, Tohoku University, Sendai. 980-8579, Japan.

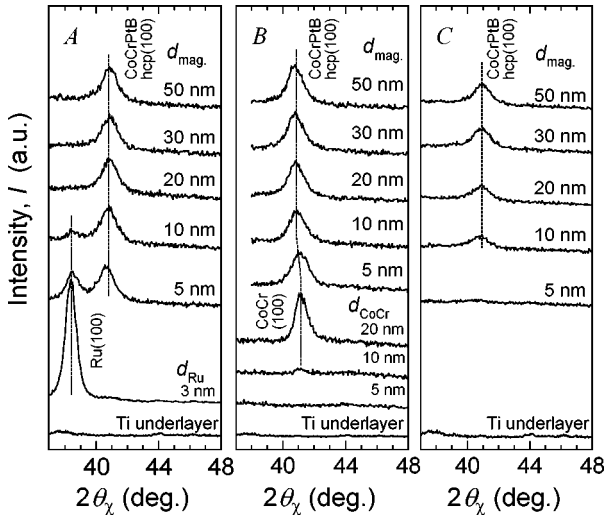

FIG. 2. In-plane XRD profiles for $Co_{69}Cr_{19}Pt_8B_4$ media with various magnetic film thickness, d_{mag}, (A) with Ru (3 nm), (B) with a $Co_{60}Cr_{40}$(20 nm)/C(1 nm) intermediate layer, and (C) without an intermediate layer, respectively. In-plane XRD profiles for Ru films deposited on a Ti underlayer (in the left figure), $Co_{60}Cr_{40}$/C film deposited on a Ti underlayer (in the middle figure), and Ti film (in the right figure) are also shown.

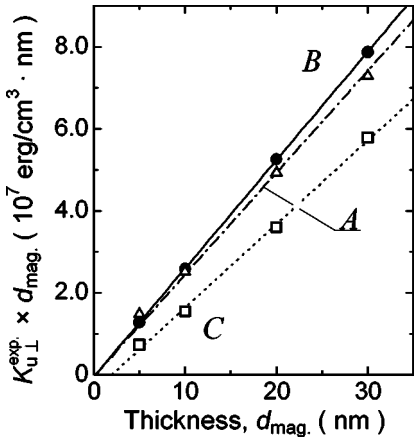

FIG. 3. $K_{u\perp}^{exp} \times d_{mag}$ vs d_{mag} plots for $Co_{69}Cr_{19}Pt_8B_4$ media (A) with Ru (3 nm) and (B) with a $Co_{60}Cr_{40}$(20 nm)/C(1 nm) intermediate layer, and (C) without an intermediate layer, respectively.

(B) $Co_{60}Cr_{40}$/C(1 nm), respectively. For the medium A with an Ru intermediate layer, both H_c and S show the maximum values of 2.8 kOe and 0.78 at $d_{inter}=3$ nm, respectively. On the other hand for the medium B with a $Co_{60}Cr_{40}$/C intermediate layer, both H_c and S show the maximum values of 3.5 kOe and 0.88 at $d_{inter}=20$ nm, respectively.

Figure 1 (right) shows the dependence of perpendicular magnetic properties H_c and S on magnetic film thickness, d_{mag}, for $Co_{69}Cr_{19}Pt_8B_4$ media with an (A) Ru(3 nm) and (B) $Co_{60}Cr_{40}$(20 nm)/C(1 nm) intermediate layer, respectively. In the same figure, H_c and S for the medium (C) without an intermediate layer are also shown for comparison. For the media C with $d_{mag} \leqslant 10$ nm, H_c and S show low values of 0.1 kOe and 0.09, respectively. On the other hand, for the media A and B, H_c and S show relatively high values of about 1.4 kOe and 0.50, respectively, even when $d_{mag}=10$ nm. Especially for the medium B, the maximum values of H_c and S are 3.5 kOe and 0.88 at $d_{mag}=30$ nm, which are higher than those of the media A.

Figure 2 shows in-plane XRD profiles for $Co_{69}Cr_{19}Pt_8B_4$ media with various magnetic film thickness, d_{mag}, (A) with Ru (3 nm), (B) with $Co_{60}Cr_{40}$(20 nm)/C(1 nm) intermediate layer, and (C) without intermediate layer, respectively. In-plane XRD profiles for Ru film deposited on a Ti underlayer (in the left figure), $Co_{60}Cr_{40}$/C film deposited on a Ti underlayer (in the middle figure), and Ti film (in the right figure) are also shown. In the profiles for a Ru (3 nm) film and a $Co_{60}Cr_{40}$ (20 nm) film, a diffracted line from the (100) plane from the hexagonal structure can be clearly seen. Therefore it was clarified that *c*-plane-oriented Ru grains or CoCr grains grow in the intermediate layer. Taking a look at the XRD patterns of the magnetic layer, it is found that for the medium C with $d_{mag}=5$ nm, a diffracted line can be hardly observed, and with increase $d_{mag} \geqslant 10$ nm, a diffracted line from the (100) plane becomes observable. This fact indicates that for the medium C, *c*-plane-oriented columnar grains grow on the initial layer, which consist of nanocrystalline grains with random orientation. On the contrary, for the media A and B with $d_{mag}=5$ nm, a diffracted line from the (100) plane can be clearly observed. Therefore it is suggested that for the media A and B, *c*-plane-oriented columnar grains in the magnetic film grow from the initial growth stage.

Figure 3 shows a $K_{u\perp}^{exp} \times d_{mag}$ versus d_{mag} plot for $Co_{69}Cr_{19}Pt_8B_4$ media (A) with Ru (3 nm), (B) with a $Co_{60}Cr_{40}$(20 nm)/C(1 nm) intermediate layer, and (C) without an intermediate layer, respectively. Judging from the intersection of the extended line of the linear portion of the $K_{u\perp}^{exp} \times d_{mag}$ curve with the d_{mag} axis, the medium C has the initial layer with the thickness of 2.0 nm. On the contrary, for the media A and B, the initial layer is completely eliminated. Based on the analyses of in-plane XRD in Fig. 2 and the $K_{u\perp}^{exp} \times d_{mag}$ plot in Fig. 3, the media A and B can be concluded to grow epitaxially. Furthermore, according to the

TABLE I. d_{ini}, K_u^{grain}, M_s, H_c/H_k, and α for $Co_{69}Cr_{19}Pt_8B_4$ medium. H_c/H_k and α are for the media with $d_{mag}=30$ nm.

	Layer structure	d_{ini} (nm)	K_u^{grain} (erg/cm^3)	M_s (emu/cm^3)	H_c/H_k (30 nm)	α (30 nm)
A	$Co_{69}Cr_{19}Pt_8B_4$/Ru (3 nm) /Ti (25 nm)	0.2	2.53×10^6	488	0.27	1.45
B	$Co_{69}Cr_{19}Pt_8B_4$/$Co_{60}Cr_{40}$ (20 nm) /C(1 mm)/Ti (25 nm)	0	2.76×10^6	477	0.30	1.35
C	$Co_{69}Cr_{19}Pt_8B_4$/Ti (25 nm)	2.0	2.04×10^6	433	0.32	1.15

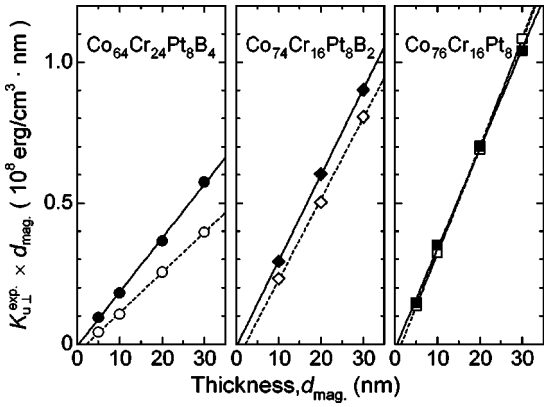

FIG. 4. $K_{u\perp}^{\exp}\times d_{\mathrm{mag}}$ vs d_{mag} plots for the media with and without the $Co_{60}Cr_{40}$(20 nm)/C(1 nm) intermediate layer for (left) $Co_{64}Cr_{24}Pt_8B_4$, (center) $Co_{74}Cr_{16}Pt_8B_2$, and (right) $Co_{76}Cr_{16}Pt_8$ media are shown in separate graphs. A closed or an open symbol corresponds to the medium with or without the intermediate layer, respectively.

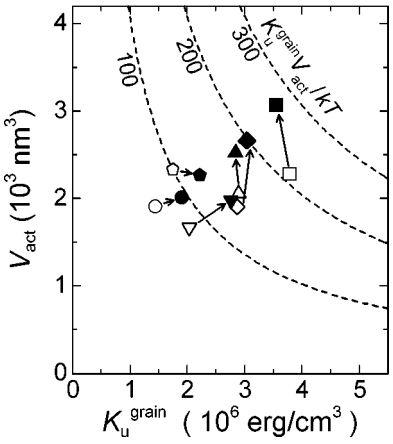

Relationship between activation volume V_{act} and uniaxial magnetocrystalline anisotropy of the columnar structure, K_u^{grain} for 30-nm-thick media. In the figure, equivalue lines of thermal stability factor, $K_u^{\mathrm{grain}} V_{\mathrm{act}}/kT$, are also drawn as a reference. An open or closed symbol corresponds to the medium with or without the $Co_{60}C_{20}$(20 nm)/C (1 nm) intermediate layer, respectively, and (●), (⬟), (▼), (♦), (▲), and (■) are represented properties for $Co_{64}Cr_{24}Pt_8B_4$, $Co_{60}Cr_{20}Pt_{16}B_4$, $Co_{69}Cr_{19}Pt_8B_4$, $Co_{74}Cr_{16}Pt_8B_2$, $Co_{64}Cr_{20}Pt_{16}$, and $Co_{76}Cr_{16}Pt_8$ media, respectively. In the figure, equivalue lines of the thermal stability factor, $K_u^{\mathrm{grain}} V_{\mathrm{act}}/kT$, are also drawn.

evaluation of the gradient of the linear portion of $K_{u\perp}^{\exp}\times d_{\mathrm{mag}}$ curves, the values of K_u^{grain} for the media A (2.53×10^6 erg/cm^3) and B (2.76×10^6 erg/cm^3) are remarkably larger than that for the medium C (2.04×10^6 erg/cm^3). Therefore for the $Co_{69}Cr_{19}Pt_8B_4$ medium, the epitaxial growth using *c*-plane-oriented Ru and a $Co_{60}Cr_{40}$/C intermediate layer enables one to increase K_u^{grain} by 24%–35%. The evaluated properties for the media A, B, and C are summarized in Table I. Comparing the medium A with B, H_c/H_k^{grain} for the medium B is larger and α is smaller than those for the medium A. This fact means that magnetic grains in the medium B is well isolated compared with that in the medium A. Hence it is suggested that the promotion of Cr segregation to the grain boundary in epitaxially grown media depends on the material of the intermediate layer.

We have further applied the epitaxial growth technique utilizing the $Co_{60}Cr_{40}$(20 nm)/C(1 nm) intermediate layer to enhance the K_u^{grain} of several perpendicular media. In Fig. 4, $K_{u\perp}^{\exp}\times d_{\mathrm{mag}}$ versus d_{mag} plots are shown with and without the $Co_{60}Cr_{40}$(20 nm)/C(1 nm) intermediate layer for $Co_{64}Cr_{24}Pt_8B_4$, $Co_{74}Cr_{16}Pt_8B_2$, and $Co_{76}Cr_{16}Pt_8$ media, separately. A closed or an open symbol corresponds to the medium with or without the intermediate layer, respectively. In the medium without a intermediate layer, a several-nm-thick initial layer exists, on the other hand for the medium using the intermediate layer, the initial layer is confirmed to be almost eliminated, hence the media with the intermediate layers are suggested to grow epitaxially. However, judging from the gradient of the linear portion of $K_{u\perp}^{\exp}\times d_{\mathrm{mag}}$ curves, the enhancement of K_u^{grain} depends on the composition of the magnetic layer.

Finally, we will discuss the thermal stability. In Fig. 5, the change in K_u^{grain} and V_{act} by epitaxial growth using a $Co_{60}Cr_{40}$(20 nm)/C(1 nm) intermediate layer is shown for CoCrPt(B) media with various compositions. A closed or open symbol corresponds to the medium with or without the intermediate layer, respectively, while (●), (⬟), (▼), (♦), (▲), and (■) represent the properties for $Co_{64}Cr_{24}Pt_8B_4$, $Co_{60}Cr_{20}Pt_{16}B_4$, $Co_{69}Cr_{19}Pt_8B_4$, $Co_{74}Cr_{16}Pt_8B_2$, $Co_{64}Cr_{20}Pt_{16}$, and $Co_{76}Cr_{16}Pt_8$ media, respectively. In the figure, equivalue lines of the thermal stability factor, $K_u^{\mathrm{grain}}V_{\mathrm{act}}/kT$, are also drawn as a reference. For all the media, utilizing an epitaxial growth technique is effective to increase $K_u^{\mathrm{grain}}V_{\mathrm{act}}/kT$. In the case of $Co_{64}Cr_{24}Pt_8B_4$, $Co_{60}Cr_{20}Pt_{16}B_4$, and $Co_{69}Cr_{19}Pt_8B_4$ media, K_u^{grain} substantially improves while an only a slight change of V_{act} was observed. On the contrary, in the case of $Co_{74}Cr_{16}Pt_8B_2$, $Co_{64}Cr_{20}Pt_{16}$, and $Co_{76}Cr_{16}Pt_8$ media, K_u^{grain} changes slightly and V_{act} drastically increases. Therefore in the media with a high concentration of B or Cr, the thermal stability is improved mainly due to an increase of K_u^{grain} rather than an enlargement of V_{act}. To clarify the origin of this phenomenon from the viewpoint of the microstructure, further study including quantity analysis concerning the existence of stacking fault and composition of the columnar grains is necessary.

[1] M. Takahashi *et al.*, IEEE Trans. Magn. **33**, 2938 (1997).
[2] K. Omote and S. Matsuno, Adv. X-Ray Chem. Anal., Jpn. **205**, 30 (1999).
[3] S. Saito *et al.*, J. Magn. Soc. Jpn. **25**, 583 (2001) (in Japanese).
[4] S. Saito *et al.*, Appl. Phys. Lett. **80**, 811 (2001).
[5] K. Yamanaka *et al.*, J. Magn. Magn. Mater. **145**, 255 (1995).
[6] S. Saito *et al.*, J. Magn. Soc. Jpn. **26**, 210 (2002) (in Japanese).
[7] S. Saito, F. Hoshi, and M. Takahashi, IEEE Trans. Magn. **38**, 1985 (2002).